Assessing Cu²⁺ active sites evolution on Cu-SSZ-13 NH₃-SCR catalysts during hydrothermal aging: A transient response approach

Umberto Iacobone [a], Nicole Daniela Nasello [a], Isabella Nova [a], Enrico Tronconi [a,*], Rohil Daya [b], Hongmei An [b], Unmesh Menon [b]

[a] *Laboratory of Catalysis and Catalytic Processes, Dipartimento di Energia, Politecnico di Milano, Via La Masa 34, Milano 20156, Italy*
[b] *Cummins Inc., 1900 McKinley Ave, Columbus, IN 47201, United States*

ARTICLE INFO

ABSTRACT

Hydrothermal aging (HTA) conditions are commonly reached in Diesel engine NH₃-SCR architectures based on Cu-CHA catalysts, altering the catalyst performance due to irreversible transformations of the catalytic sites. Relying on transient response methods (TRMs), we study two Cu-SSZ-13 samples with different HTA extents. The following conclusions apply: i) the Cu²⁺content is invariant with HTA; ii) the $ZCu^{2+}(OH)^-$ population decreases concurrent to the increase of the Z_2Cu^{2+} fraction and to iii) the loss of Brønsted acidity. This evidence agrees with the simple stoichiometry proposed for mild HTA processes: $ZCu^{2+}(OH)^- + ZH^+ \rightarrow Z_2Cu^{2+} + H_2O$. Furthermore, TRMs permit to observe additional phenomena which comply with a low-T Cu²⁺-pair mediated reduction pathway recently proposed. The results from a comprehensive set of simple experimental flow reactor methods consolidate the proposed aging mechanism, strengthen the SCR reduction half cycle (RHC) mechanistic understanding and showcase TRMs as a viable alternative to more complex techniques for the characterization of Cu-CHA catalysts.

1. Introduction

Nitrogen oxides (NOx) have long been recognized as harmful species, contributing to a reduction of the life expectancy and to air pollution phenomena such as photochemical smog, acid rains and greenhouse effect [1–3]. Vehicular fossil fuel combustion acts as a prominent emission source, and growing aftertreatment performance requirements are necessary to progressively reduce their release [2,3]. The Selective Catalytic Reduction of NOx with NH₃/urea (NH₃-SCR) is currently the state-of-the-art technology to comply with this need for Diesel and heavy-duty lean burn engines applications and, in the last decade, small pore Cu-promoted zeolites have emerged as the SCR catalyst-of-choice. Indeed, the chabazite topology (Cu-CHA) has shown a remarkable hydrothermal stability and resistance to hydrocarbon poisoning, combined with a superior deNOx activity, low N₂O selectivity and contained NH₃ slip with respect to other frameworks [4–11]. During the low-temperature (low-T) SCR regime (<250°C), a reversible transformation of the Cu ions oxidation state has been proposed to occur (Cu²⁺ ↔ Cu⁺) according to a redox chemistry. The overall mechanism can be decoupled in two parts, which comprises a reduction (RHC: Cu²⁺ → Cu⁺) and an oxidation (OHC: Cu⁺ → Cu²⁺) half-cycle. However, the exact nature of these processes is still controversial [12–14].

The existence of two different isolated Cu²⁺ cations inside the zeolite crystalline structure, namely $ZCu^{2+}(OH)^-$ and Z_2Cu^{2+}, has been extensively probed, on both model and commercial Cu-CHA catalysts, with a variety of techniques (e.g. DRIFTS, in situ FTIR, DFT, H₂-TPR) [5, 15–19]. Different position, reducibility and mobility have been attributed to these two species: the double coordination with the proximate framework-Al (Z) inside the 6-member ring plane of the CHA cage confers to Z_2Cu^{2+} the highest thermodynamic stability, while $ZCu^{2+}(OH)^-$, characterized by a single bond with the zeolite structure in the 8-membered window, results in enhanced reducibility. The initial populations of the two ions have been proved to depend on the catalyst composition, i.e., on the Cu/Al and Si/Al ratios [15,17,18], however real-world phenomena may activate additional dynamic changes of their nature. Hydrothermal aging (HTA) and sulfur poisoning are nowadays regarded as the main degradation sources for catalyst performance, concurrent with alterations of the active acid centers. HTA results a more complex subject, being an intrinsically irreversible phenomenon which can induce destructive changes in the catalyst microporous

---

structure, whereas sulfur poisoning has been proved to be mostly reversible utilizing cyclic high temperature (high-T) treatments [20–25]. The typical NH$_3$-SCR thermal operative window ranges between 200~400°C, however for several after-treatment architectures, the catalysts can be periodically exposed to high temperatures (>600°C) in an environment rich in water and oxygen, typically during the Diesel Particular Filter (DPF) and SCR deSOx regeneration processes, thus enabling catalyst hydrothermal aging (HTA) activation conditions [26]. The robust chabazite structure can withstand harsh conditions (>800°C) with limited structural damages, however unavoidable loss in performance is observed [5,26–28]. Cu-SSZ-13 catalysts, widely employed in mobile NH$_3$-SCR applications, have been extensively investigated in the literature through experimental campaigns to also unveil the effect of HTA on the deNOx activity of progressively aged samples. Considering mild aging conditions (<650/700°C), converging outcomes have been reported from the application of transient tests (NH$_3$-TPD, H$_2$-TPR), surface area/micropore volumes measurements (BET, t-plot) and spectroscopic analysis (ICP, DRIFTS, Al solid-state NMR, XRD, EPR) [5,16, 18,28,29]. A conservation of the textural properties has been observed, alongside with a negligible to scarce dealumination or formation of CuO$_x$ species. The major reported event under this thermal regime is the irreversible transformation of ZCu^{2+}(OH)$^-$ ions into Z$_2$Cu^{2+}, migrating from the 8- to the 6-membered ring location, accompanied by the consumption of framework ZH$^+$ [5,16,18,28,29]. Such a conversion of Cu^{2+} cations has been rationalized by the following simple global chemistry (1) [5,18,23,28,29]:

$$ZCu^{2+}(OH)^- + ZH^+ \rightarrow Z_2Cu^{2+} + H_2O \qquad (1)$$
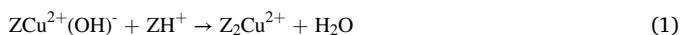
Nevertheless, the quantification of the different Cu^{2+} ions results challenging, typically relying on signals deconvolution affected by the overlap of multiple peaks and/or by the selection of reference spectra (NH$_3$-TPD, H$_2$-TPR, XANES, EPR) [5,18,23,30,31].

In this context, the present work showcases a viable alternative to such techniques. A combination of simple, yet effective, transient response methods (TRMs) previously developed [17,32–38] has been herein applied to directly interrogate the mild-aging mechanism (1) and to assess the Cu^{2+} cations population over two differently aged state-of-the-art Cu-SSZ-13 catalysts. The overall content of reducible Cu^{2+} has been quantified by NO+NH$_3$ reduction tests. Successive NO$_2$ and NH$_3$ adsorption + TPD experiments permitted to evaluate the evolution of the catalyst sites speciation, with the former protocol providing a straightforward assessment of the ZCu^{2+}(OH)$^-$ cations requiring no peak deconvolution. Additionally, the Cu^{2+} nuclearity during conditions representative of the low-T RHC has been investigated by transient CO to CO$_2$ oxidation tests, with the purpose to probe the formation of multinuclear Cu^{2+} species in such environment as well as the related aging effect. The results of such a transient methodology comply well with the probed chemistry, validating its application to investigate the temporal evolution of the catalyst structure during aging phenomena.

2. Material and methods

2.1. Catalyst samples and experimental rig

Samples from two aging conditions of a state-of-the-art Cu-exchanged chabazite catalyst (Cu-SSZ-13), provided by Cummins Inc., have been used to investigate the chemistry underlying the HTA phenomena. As discussed in the *Introduction*, HTA conditions for SCR Cu-CHA catalysts are achieved in an environment rich of oxygen and water, where temperature and exposure time are the main factors controlling the extent of the aging process [5,16,18,23,26,28]. The catalysts, initially in the form of wash-coated monoliths, have been exposed to a humidified mixture containing 10% v/v O$_2$, 8% v/v CO$_2$ and 7% v/v H$_2$O diluted in nitrogen, at different controlled conditions to reach net

distinct aging levels [29]. Accordingly, the two catalysts used for this study are characterized by different aging treatments: i) a *Degreened* sample: 550°C for 4 h; ii) an *Aged* sample: 650°C for 50 h, representative for the aging conditions of an End of Useful Life catalyst [28]. Previous works have demonstrated that these hydrothermal treatments guarantee an effective change in the Cu^{2+} speciation (ZCu^{2+}(OH)$^-$, Z$_2$Cu^{2+}), with negligible Cu clusters formation and zeolitic framework damages [16, 18,28]. After this controlled aging phase, two monolith cores per sample have been extracted from the original honeycomb structure at different axial locations. The catalytic washcoat layer was separated from each core by manual scratching, and the powders from the same sample were mixed. This simple procedure allows to mediate the aging, accounting for possible non-uniformities across the original monoliths. Heating (120°C), sieving and reheating (120°C) of the mixed powders allowed to reach an average particle size of 90 μm, removing moisture and impurities from the scratching process. An independent ICP-MS analysis evaluated a Cu fraction of 2.4% w/w and negligible Mg content, confirming the absence of unwanted cordierite from the monolith scratching.

Each dry powder (32 mg), diluted with dry cordierite (up to 130 mg) with the same mean particle size, has been loaded in a vertical micro-flow quartz reactor (ID – 6 mm), placed in an electrical oven. Extensive information of the experimental set-up can be found in earlier works [7,17,33–36]. In summary, a K-type thermocouple was embedded in the catalytic bed, suspended in the quartz tube by layers of quartz wool, to track and regulate the thermal evolution of the system. The gas species were dosed by dedicated mass flow controllers (Brooks Instruments), with Helium and Argon respectively as carrier and marker; conversely an electrically heated saturator permitted the H$_2$O feed regulation. A pair of 6-way pulse valves enabled a fast reactants injection into the reactor through capillaries, while the outlet gas mixture was analyzed by a mass spectrometer (QGA Hiden Analytical) in parallel to a combination of a UV+IR analyzers (ABB: LIMAS11 HW + URAS26).

2.2. Experimental protocols: TRMs

Prior to each test, a 1-hour pre-treatment phase at high temperature (550°C) with 8% v/v of O$_2$ was executed to clean the catalyst from any lingering adsorbed species and complete the Cu re-oxidation (Cu$^+$ → Cu^{2+}). This latter aspect is particularly relevant and has been extensively verified [17,32–36,38]. The system was then cooled down in the same oxidative gas mixture, till reaching the target temperature; when water was required, it was fed in the proximity of the operative temperature. Three different experimental protocols, carried out at a constant gas hourly space velocity (GHSV) of 266250 cm^3/h/g$_{cat}$ (STP), have been herein utilized: they are briefly recalled in the following, being thoroughly described elsewhere [17,32–35,37–39].

Isothermal NO+NH$_3$ reduction tests at 200°C allowed to titrate the catalyst reducible Cu^{2+} content [17,23,28,32,33,35,40–43]. Two different protocols have been employed, with details reported in the Supporting Information (FigSI.1). The reactants co-feed phase (500 ppm) was the cardinal element for both, wherein the observed NO consumption and N$_2$ production were ascribed to the copper reduction. The resulting transient profiles were affected by the catalyst treatment prior to the NO+NH$_3$ injection: *Protocol A* (FigSI.1 – A) included a NH$_3$ pre-saturation phase in the presence of O$_2$ alongside with a scarce to negligible NH$_3$ oxidation, while 1-hour NO exposure was realized during *Protocol B* (FigSI.1 – B). Both have been realized in the presence and absence of H$_2$O (5% v/v), to assess the water impact.

The investigation of the Cu-CHA active centers was performed by isothermal adsorption tests, followed by temperature programmed desorption (TPD). Two probe molecules, namely NO$_2$ and NH$_3$, have been employed due to their distinct capability to bond with catalyst sites, enabling the Cu^{2+} speciation (ZCu^{2+}(OH)$^-$, Z$_2$Cu^{2+}) assessment [17,18,28,29,33,34,42]. Concerning the NO$_2$ tests, an initial isothermal adsorption (500 ppm) at 150°C was realized till complete catalyst

saturation, accompanied by NO production reflecting the nitrogen dioxide adsorption chemistry. After 90 min, a pure-Helium purge was realized to remove the weakly adsorbed species. Subsequentially, the temperature was increased to 550°C, at a fixed heating rate (15°C/min), to enable the desorption of the chemisorbed species. The same protocol has been applied also for NH_3, where no other species have been detected throughout the experiment, besides a small N_2 production during the TPD which was associated to the Cu^{2+} reduction by NH_3. These adsorption experiments have been carried out without H_2O in the feed stream, since water is known to inhibit both nitrates formation (during the NO_2 exposure) and NH_3 adsorption. Also, H_2O potentially activates hydrolysis processes, thus affecting the site quantification [34, 36,44].

Isothermal CO oxidation, with/without H_2O feed, has been utilized to probe the generation of multinuclear Cu species under conditions representative of the low-T RHC-SCR [34,37–39]. These multiple-step tests have been carried out isothermally at 200°C: after a 1-hour NH_3 feed to pre-saturate the catalyst (500 ppm), a purge was realized and, successive to the oxygen removal, 1000 ppm of CO were added to the feed. The CO_2 production herein observed was indicative of a Cu-pair mediated Cu^{2+} reduction pathway. Lastly, a final $NO+NH_3$ reduction phase was realized to verify the previous Cu^{2+} reduction extent and close the Cu ions balance.

3. Results and discussion

3.1. Reducible Cu^{2+} titration

3.1.1. NO+NH₃ reduction with NH₃ pre-adsorption

Different isothermal NO + NH_3 reduction protocols have been considered to investigate the hydrothermal aging effect on the quantification of Cu^{2+} sites and on their reduction dynamics. Fig. 1 depicts the reactant's co-feed phase, successive to an ammonia pre-storage step (*Protocol A*).

In the absence of H_2O in the feed (Fig. 1 – A), upon co-feeding the reactants an evident complete NO consumption, alongside with a corresponding 500 ppm N_2 release peak, is detected over both samples. Subsequently, a rapid monotonic NO increase up to the feed concentration level after ~1000 s is observed, concurrent to a mirror-like nitrogen trend approaching zero-level. Similar features are observed when H_2O is present the feed stream (Fig. 1 – B), however with an apparent lower rate of nitrogen production and NO consumption. This behavior is consistent with the well-known Cu^{2+} reduction process: in agreement with the literature [17,32–35,42,45], the process occurs consuming NO (and NH_3) while releasing N_2 with a global equimolar stoichiometry (Cu^{2+}:NO:N_2=1:1:1). Hence, a straightforward evaluation of the reducible copper is enabled by direct signals integration: Table 1 reports

Table 1
NO consumption, N_2 production and Cu^{2+} quantification according to the NO+NH_3 titration with *Protocol A*.

Protocol	Sample	NO cons., μmol	N₂ prod., μmol	NO/N₂	Cu²⁺ mean, μmol	Cu²⁺ mean, w/w %
Dry	*Degreened*	11.5	11.0	1.05	11.3	2.2
	Aged	11.8	12.0	0.98	11.9	2.4
Wet	*Degreened*	12.2	12.3	0.99	12.3	2.4
	Aged	12.0	12.6	0.95	12.3	2.4

the corresponding quantitative analysis. As shown, the NO to N_2 ratio agrees with the considered chemistry resulting close the theoretical unit value. The consequent titrated Cu^{2+}, computed as the mean average of the integrated signals, results close to the ICP-measured 2.4% w/w (with and w/out H_2O), confirming the conservation of the overall Cu cations implied by the HTA mechanism under investigation (1). Such a result is coherent with previously reported findings, based on ICP-MS, H_2-TPR, and NO+NH_3 titrations of differently aged Cu-promoted zeolites [18,28, 33,34,42,43]. The only minor deviation is observed on the *Degreened* sample under dry conditions, where a Cu fraction of 2.2% w/w was measured. While this discrepancy may be associated with experimental errors, we do not rule out a greater accuracy of the NO+NH_3 titration once water is present in the feed stream, which may inhibit unwanted catalyst reduction by the preadsorbed NH_3. Closely superimposed NO and N_2 evolutions are detected over the two catalysts, as already observed in the absence [33,34] and in the presence of H_2O feed [43]. Thus, both the Cu^{2+} quantification and the reduction dynamics can be inferred to be insensitive to the catalyst hydrothermal pre-treatments, and to the consequent change of the Cu^{2+} speciation ($ZCu^{2+}(OH)^-$, Z_2Cu^{2+}), in the presence of an NH_3 pre-saturation phase.

The scarce Cu^{2+} speciation effect in similar reaction conditions has been proposed in the DFT work of Paolucci et al. [19] who estimated similar activation barriers over the two isolated Cu^{2+} cations. In close relation, a recent kinetic analysis of Cu^{2+} reduction transients by Deka et al. [41] resulted in similar kinetics for both species. The nuclearity of the low-T SCR-RHC catalytic active centers remains nowadays a debated subject in the literature. While popular mechanisms are based on single-site interpretations [12,19,45] an alternative Cu^{2+}-pair NO-activated reduction pathway has been recently proposed, based on converging experimental, theoretical and kinetic evidence [32–35,38, 39]. The proposed chemistry complies well with the observations herein reported and with the CO oxidation tests later discussed in the manuscript, thus its main characteristics are here recalled. As well documented, once ammonia coordinates on Cu^{2+} ions, at least two differently NH_3-solvated complexes are formed, namely $Cu^{2+}(OH)^-(NH_3)_3$ and
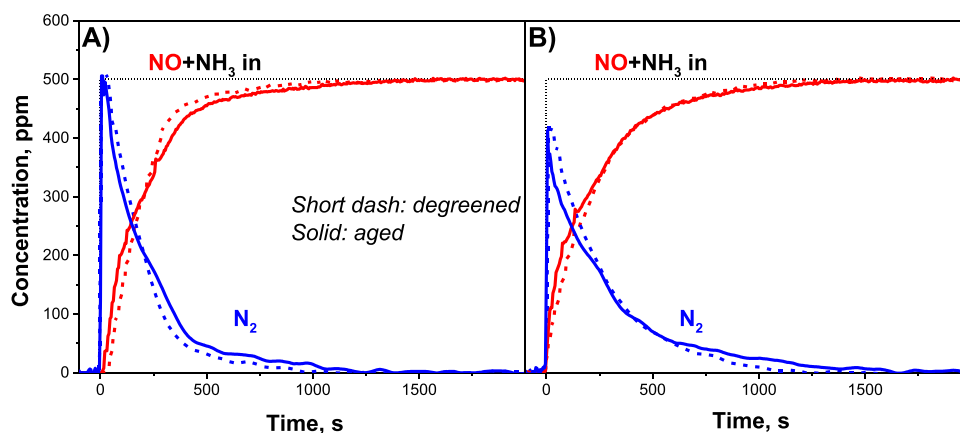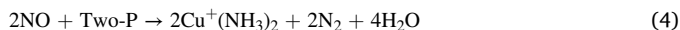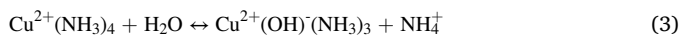

Fig. 1. Temporal evolution of NO and N_2 with *Protocol A*, without (A) and with (B) a constant H_2O feed, during the NO+NH_3 reduction step. Gas phase composition: NO = NH_3 = 500 ppm, O_2 = 0 % v/v, H_2O = 0 – 5 % v/v, balance He. GHSV = 266250 $cm^3/h/g_{cat}$ (STP) (W_{cat} = 32 mg). T = 200 °C.

$Cu^{2+}(NH_3)_4$, detached from the framework and characterized by different degrees of mobility inside the zeolite crystalline structure, respectively being inter- and intra-cage mobile [12,13,17,19,32,46,47]. Under these conditions, DFT has shown the feasibility of an exergonic coupling of two $Cu^{2+}(OH)^-(NH_3)_3$ complexes, forming a proximate structure labeled as Two-P (i.e., $Cu^{2+}(OH)^-(NH_3)_3 \bullet \bullet \bullet Cu^{2+}(OH)^-(NH_3)_3$), reaction (2):

$$Cu^{2+}(OH)^-(NH_3)_3 + Cu^{2+}(OH)^-(NH_3)_3 \leftrightarrow Two\text{-}P \quad (2)$$
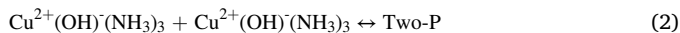
Such a process drives thermodynamically the reversible $Cu^{2+}(NH_3)_4$ hydrolysis (3). Ultimately NO, acting as the Two-P scavenging element, enhances the sites hydrolysis favoring the complete conversion into $Cu^{2+}(OH)^-(NH_3)_3$ (4).

$$Cu^{2+}(NH_3)_4 + H_2O \leftrightarrow Cu^{2+}(OH)^-(NH_3)_3 + NH_4^+ \quad (3)$$

$$2NO + Two\text{-}P \rightarrow 2Cu^+(NH_3)_2 + 2N_2 + 4H_2O \quad (4)$$

Indeed, a similar activation barrier has been assessed for (3) and (4), suggesting the two steps to proceed concurrently [34]. This mechanistic interpretation explains the observed negligible HTA effect on the transient catalyst reduction dynamics, since the Cu^{2+} sites hydrolysis, step (3), grants identical behavior to the catalysts, regardless of the Cu^{2+} speciation.

Concerning the H_2O effect on the low-T RHC, while a negligible impact on the integral Cu^{2+} titration can be inferred, inhibition of the reduction dynamics is clearly observed. The work of Gramigni et al. [33] reported similar features over two different model Cu-CHA catalysts in the presence of 2% v/v H_2O. In addition, recent research has shown multiple effects of water vapor on the Fast and Standard SCR activity, depicting a complex dependency on both the NO_x concentration, temperature and H_2O concentration [48]. A very recent DFT study has provided a theoretical interpretation for the H_2O inhibition observed during reduction of Cu^{2+} cations in Cu-CHA catalysts: the entropic penalties resulting from the presence of H_2O molecules in the chabazite cage more than compensate the positive enthalpic stabilization of the RHC transition state, thus explaining the observed inhibition effect [49].

3.1.2. NO+NH₃ reduction without NH₃ pre-adsorption

After collecting evidence of the negligible HTA effect on the RHC in the case of NH₃-saturated catalysts, the investigation has been extended to address the lack of preadsorbed NH₃. This case has been analyzed supplying a delayed NH₃ feed, successive to the NO feed: this protocol (Protocol B) has been applied over both catalyst samples, with and without H_2O, and the corresponding RHC phases and quantitative analysis are shown in Fig. 2 and Table 2.

The observed features resemble those of Fig. 1, namely a N₂

Table 2
NO consumption, N₂ production and Cu^{2+} quantification employing the NO+NH₃ titration with Protocol B.

Protocol	Sample	NO cons., μmol	N₂ prod., μmol	NO/ N₂	Cu^{2+} mean, μmol	Cu^{2+} mean, w/w %
Dry	Degreened	11.4	11.1	1.03	11.3	2.2
	Aged	11.5	11.5	1.00	11.5	2.3
Wet	Degreened	12.0	11.6	1.03	11.8	2.3
	Aged	11.8	11.3	1.04	11.6	2.3

production with a mirror-like NO consumption and an integral equimolar proportion between the two. This is still representative of the Cu^{2+} reduction occurrence and, utilizing the known copper cations reduction stoichiometries [17,32–35,42,45], we quantify a similar loading on both samples ∼2.2/2.3% w/w, regardless of both the HTA level and the water presence. Such a titration, despite being close to the reference value 2.4% w/w, recurrently underestimates it albeit slightly. This loss could be ascribed to a modest copper reduction by NO during the step preceding the NH₃ feed, as observed in the literature [32], thus lowering the oxidized copper fraction available during the successive titration phase. Alternatively, NO and NH₃ may react with $ZCu^{2+}(OH)^-$ pairs to form small traces of gas-phase NO₂, here not observed due to adsorption on the catalyst. This poses Protocol B as less reliable than Protocol A for the Cu^{2+} titration. Further discussion of this aspect is provided in the Supporting Information (Section SI1).

A major difference introduced by the application of this protocol, with respect to the NH₃ pre-saturation case, is observed for the signal's dynamics. Upon ammonia dosing, a plateau-like feature (∼100 ppm) for both NO and N₂ is now observed, followed by the gradual completion of the reduction. This behavior was shared by both samples, however the initial constant consumption phase appeared more noticeable on the Degreened catalyst. Similar reduction dynamics features have been already noted in the literature, both on model catalysts in the absence of water [32,33] and on commercial samples in the presence of a wet feed stream (7% H_2O v/v) [41,43]. Since no NH₃ is initially available, the plateau trait can be considered the result of consecutive processes: the slow progressive NH₃ solvation of the Cu^{2+} ions limited their reduction [32,33,41,43]. Noteworthily, in the considered protocol H_2O scarcely affects the signal dynamics (Fig. 2 – B) and the previously assessed inhibition effect on the transient signal profiles is not detected here, consistent with the Cu^{2+} reduction not being rate limiting in this protocol.
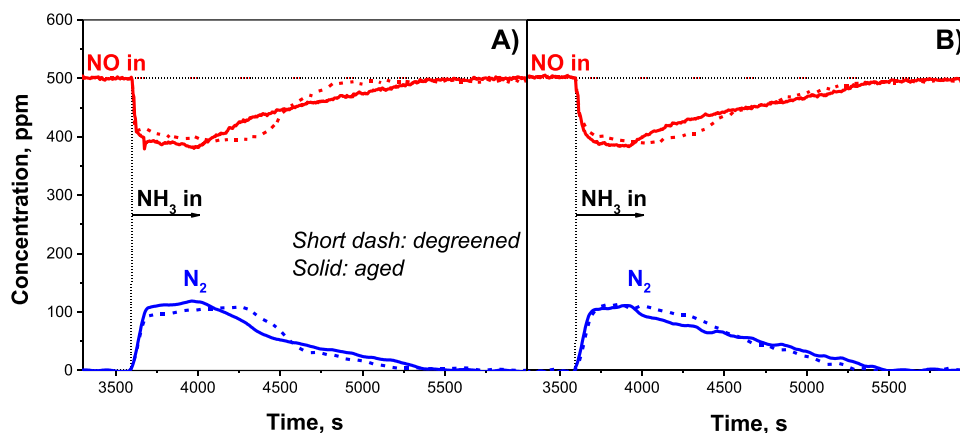

Fig. 2. Temporal evolution of NO and N₂ with Protocol B, without (A) and with (B) a constant feed of water, during the NO+NH₃ reduction step. Gas phase composition: NO = NH₃ = 500 ppm, O_2 = 0 % v/v, H_2O = 0 – 5 % v/v, balance He. GHSV = 266250 cm³/h/g$_{cat}$ (STP) (W$_{cat}$ = 32 mg). T = 200 °C.

3.2. Cu^{2+} speciation and Brønsted acidity

3.2.1. NO$_2$ adsorption + TPD

The chemistry involved in the Cu^{2+} quantification examined in the previous section does not allow to discriminate between the cations populations of different catalysts, requiring the adoption of a different approach to study the evolution of the catalyst speciation during HTA. Nitrogen dioxide adsorption, followed by a TPD, has been recently proposed as a straightforward flow reactor method to evaluate the ZCu^{2+}(OH)$^-$ content of Cu-CHA catalysts, showing a remarkable consistency across different TRMs affected by the Cu^{2+} speciation [17,33, 34,36,38]. Negri et al. [44] demonstrated, through the application of spectroscopic techniques, that NO$_2$ is stored only on ZCu^{2+}(OH)$^-$ ions according to a disproportion mechanism releasing NO, as follows [17, 44,50]:

$$2ZCu^{2+}(OH)^- + 3\,NO_2 \rightarrow 2ZCu^{2+}NO_3^- + NO + H_2O \qquad (5)$$
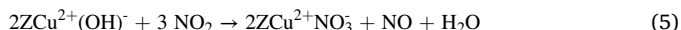
In the subsequent TPD phase, the Cu-nitrates are expected to decompose releasing NO$_2$. Eq. (5) thus enables direct quantification of ZCu^{2+}(OH)$^-$ cations by integrating either the NO evolution or the NO$_2$ release during the adsorption or TPD steps, respectively. With this purpose, a dedicated experimental protocol has been applied: Fig. 3 shows the signals evolution during the NO$_2$ adsorption phase (A) and the corresponding TPD (B), for both the investigated catalysts.

As soon as NO$_2$ reaches the catalyst, an NO peak is observed, followed by a rapid drop to the zero-level while NO$_2$ approaches the feed concentration, saturating the catalyst. Successive to an isothermal desorption phase, to enable the removal of weakly adsorbed species, a controlled temperature ramp is realized, to induce the desorption of chemically adsorbed species and an NO$_2$ peak is detected. These features reconcile well with the NO$_2$ adsorption chemistry (5) and the HTA mechanism previously considered (1). As the ZCu^{2+}(OH)$^-$ ions are converted into Z$_2$Cu^{2+} upon aging, a decrease in the nitrates formation is expected, lowering the extent of the NO$_2$ adsorption process. The *Aged* catalyst in fact features a reduced NO production and a faster NO$_2$ saturation with respect to the *Degreened* sample, in close agreement with the lower NO$_2$ trace during the TPD. These outcomes are consistent with previous works on Cu-CHA catalysts where alterations in the adsorption/desorption features were attributed to different ZCu^{2+}(OH)$^-$ ions contents, both on model samples with similar HTA conditions or on model and commercial ones aged to different extents [17,33,42]. The integration of the relevant signals is reported in *TableSI.2*, indicating a modest experimental error in the N-balances (~5%). The main results are shown in Table 3, where the expected equimolar ratio between the NO$_2$ released (in the TPD) and twice the NO produced (in the NO$_2$ adsorption phase) further supports the considered mechanism (5). With

Table 3
NO production, NO$_2$-TPD release and evaluation of the Cu^{2+} speciation (ZCu^{2+}(OH)$^-$, Z$_2$Cu^{2+}) using NO$_2$ adsorption at 150°C + TPD protocol.

Sample	NO prod., μmol	NO$_2$ TPD, μmol	$\dfrac{NO_2 TPD}{2 * NO\ prod}$	ZCu^{2+}(OH)$^-$, %	Z$_2$Cu^{2+}, %
Degreened	4.8	9.0	0.94	75.0	25.0
Aged	2.4	4.7	0.98	39.0	61.0

the knowledge of the total reducible Cu^{2+} from previous tests, ZCu^{2+}(OH)$^-$ fractions of 75% and 39% are respectively estimated for the *Degreened* and the *Aged* sample. The ZCu^{2+}(OH)$^-$ population predominancy in the *Degreened* sample is in fact coherent with literature reports for fresh, or mildly aged, high metal-loading Cu-promoted chabazite catalysts [5,18,19,23,30,31]. Furthermore, similar Cu^{2+} speciation estimates over similarly aged Cu-SSZ-13 catalysts have been reported based on signals deconvolutions or model predictions [23,42]. The net reduction in the ZCu^{2+}(OH)$^-$ content over the *Aged* sample is also in agreement with EPR measurements and kinetic modeling procedures [5, 42]. Since no specific TRMs are currently available for the direct titration of Z$_2$Cu^{2+} alone, it has been tentatively evaluated as the complement of the estimated ZCu^{2+}(OH)$^-$ population.

To further investigate the stability of the ZCu^{2+}(OH)$^-$ population, NO$_2$-adsorption/TPD tests have been replicated at the end of the experimental campaign: the respective TPD results over both catalysts (*red curves*), compared to the reference ones (*black curves*), are displayed in Fig. 4.

Almost superimposed NO$_2$ desorption profiles are observed over both catalysts. Furthermore, with respect to the reference titration results reported in Table 3, negligible variations are found. The reproductions are indeed characterized by an integral TPD release of 9.2 and 5.0 μmol, respectively for the *Degreened* and the *Aged* sample, thus with a marginal change of 0.2/0.3 μmol well within the experimental error of the experimental measurements. Interestingly, the *Degreened*-TPDs show an evident single feature, in agreement with the presence of one adsorption site for NO$_2$; on the *Aged* counterpart a similar, although less pronounced, peak is apparent in the replicated test, while a more complex, bimodal feature is noted in the initial test. We speculate that this may be related to an initial evolution of the ZCu^{2+}(OH)$^-$ cations acting as NO$_2$ adsorption sites, since the reference NO$_2$ adsorption/TPD tests were carried out early in the experimental campaign, immediately after the HTA treatment. Overall, however, a net stability of the Cu^{2+} speciation can be inferred from these tests, particularly when hydrothermal aging conditions are not applied. Notably, no lingering effects of different reaction environments and processes (e.g. oxidation, reduction, NH$_3$ solvation and coupling of Cu ions) are observed: a stable ZCu^{2+}(OH)$^-$ population is recovered after all the experiments.

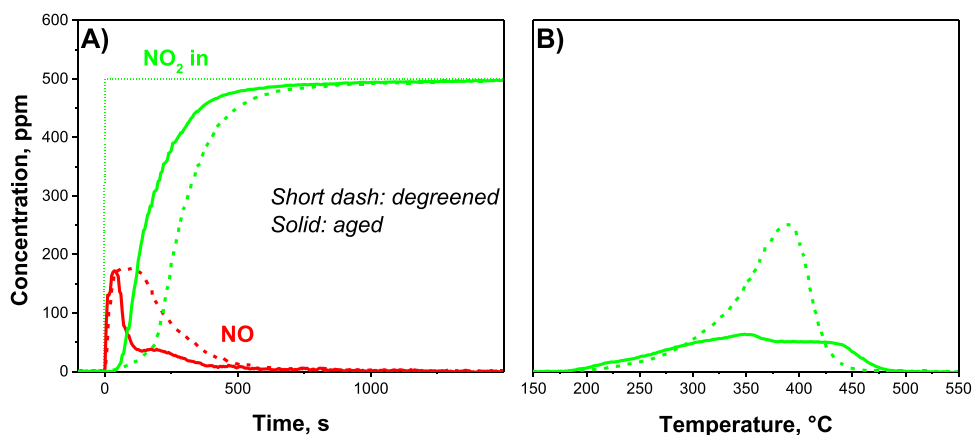**Fig. 3.** NO$_2$ adsorption and NO production during the NO$_2$ adsorption phase at 150°C (A), and TPD step (B). Gas phase composition: NO$_2$ = 500 − 0 ppm, O$_2$ = 0 % v/v, H$_2$O = 0% v/v, balance He. GHSV = 266250 cm^3/h/g$_{cat}$ (STP) (W$_{cat}$ = 32 mg). T = 140 − 550°C, heating rate = 15 °C/min.
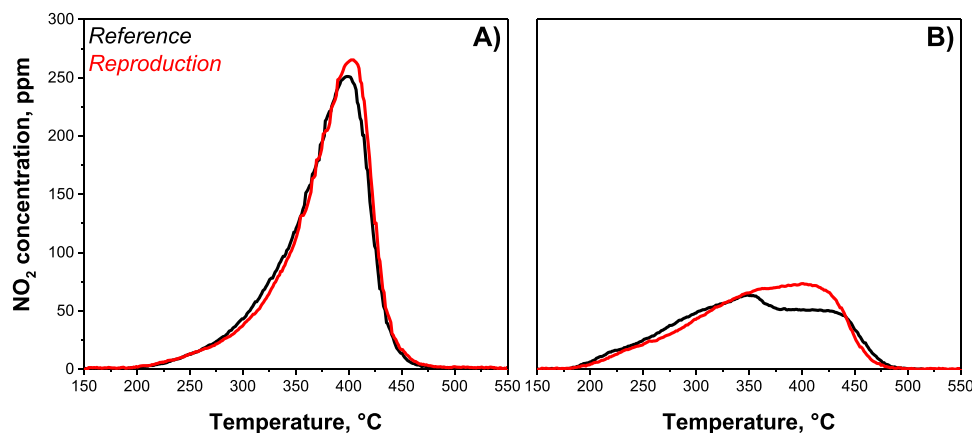
Fig. 4. NO$_2$-TPD comparison between the reference (black) and the reproducibility test at the end of the experimental campaign (red), for the *Degreened* (A) and the *Aged* (B) samples. Gas phase composition: He-only. GHSV = 266250 cm^3/h/g$_{cat}$ (STP) (W$_{cat}$ = 32 mg). T = 140 – 550°C, heating rate = 15 °C/min.

3.2.2. NH$_3$ adsorption + TPD

Ammonia is a well-known probe molecule extensively used in the literature to assess catalyst acidity modifications, establishing NH$_3$ adsorption/TPD as a valid tool to be associated with the previous NO$_2$-based protocol. Indeed, the NH$_3$ capacity to interact with the variety of zeolite acid sites, forming bonds characterized by different binding energies, guarantees facile detection of a variety of phenomena. Catalyst aging, sulfur and hydrocarbon poisoning, as well as the catalyst composition (*e.g.*, Cu loading, SAR, framework) have been typically evaluated in the literature by NH$_3$-TPD analysis, following isothermal adsorption steps [16–18,28,36,42,51]. As previously discussed, gas-phase ammonia has been proven to solvate the two Cu^{2+} cations differently, respectively forming fully coordinated species with 3 and 4 ligands (Cu^{2+}(OH)$^-$(NH$_3$)$_3$ and Cu^{2+}(NH$_3$)$_4$) [12,17,19,42,46,47]. Nevertheless, the removal of gaseous NH$_3$ from the reacting environment determines the desorption of weakly adsorbed NH$_3$, with a decrease of the NH$_3$ coordination to 1 and 2, respectively. The proposed remaining complexes are Cu^{2+}(OH)$^-$(NH$_3$) and Cu^{2+}(NH$_3$)$_2$, major constituents of the Lewis-NH$_3$ desorbed during the TPD phase [17–19, 36,42]. Being affected by the Cu^{2+} speciation, Lewis-NH$_3$/Cu^{2+} ratios have been often utilized as indexes to represent changes in the relative cation's population [17,18,36]. Besides copper, the framework Brønsted acid sites (ZH$^+$) are likewise involved in the adsorption process, being bound to at least one NH$_3$ molecule each (ZNH$_4^+$); minor to negligible weak ammonia coordination on extra-framework Al could additionally occur.

With the intent to observe the Brønsted sites evolution upon aging and to cross-check the previously assessed Cu^{2+} speciation, NH$_3$ adsorption/TPD tests have been carried out in a similar manner to the NO$_2$ runs, with the TPD steps shown in Fig. 5 – A for both catalysts. During this thermal desorption phase, concurrent to the NH$_3$ release, a small N$_2$ trace was detected whose integral production is reported in Table SI.3. It is ascribed to the NH$_3$ ability to reduce Cu^{2+} at high temperature, thus releasing nitrogen following a 1:6 stoichiometry with respect to copper, as confirmed both by spectroscopic and TRM evidence [36,52,53]. As this occurrence implies consumption of NH$_3$, a proper TPD evaluation requires accounting for this contribution (*i.e.*, NH$_3$ + 2*N$_2$). The small N-balance errors (~4%) evaluated for these tests (Table SI.3) validate the analysis adequacy.

The well-resolved bimodal NH$_3$-TPD curve is a known feature for the Cu-CHA-catalysts: it is commonly accepted that the low-T feature is mainly ascribed to the Lewis-NH$_3$ release from Cu^{2+}(OH)$^-$(NH$_3$)$_3$ and Cu^{2+}(NH$_3$)$_4$, while the high temperature peak is associated with the release from stronger Brønsted acid sites [7,17,18,28,36]. A net change in the peaks' magnitude is evident upon aging, where the *Aged* sample shows an evident enhancement in the Lewis sites, in conjunction to a loss of the high-T feature with respect to the *Degreened* catalyst. In addition, the overall NH$_3$ storage is found to remain almost the same, as shown in Table SI.3, suggesting an overall integrity of the zeolite framework under mild hydrothermal aging conditions, in agreement with the literature [5,16,18,28]. Both pieces of evidence agree with the HTA mechanism (1): a rising Z$_2$Cu^{2+} population, capable to bind more NH$_3$ molecules than ZCu^{2+}(OH)$^-$, determines an increment in the Lewis acidity. Concurrently, Brønsted sites are consumed, leading to the decrement of the high-T feature. Indeed, the newly formed Z$_2$Cu^{2+} can coordinate two NH$_3$ molecules, balanced by the consumption of
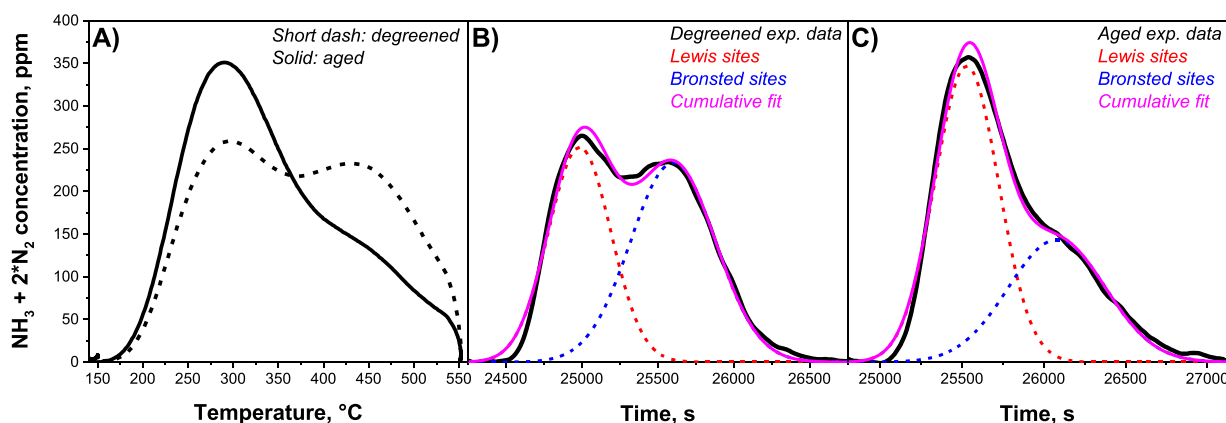

Fig. 5. NH$_3$ release (NH$_3$+2*N$_2$) during the TPD phase (A) and the respective deconvolution for the *Degreened* (B) and *Aged* (C) catalysts. Gas phase composition: NH$_3$ = 0 ppm, O$_2$ = 0 % v/v, balanced in He. GHSV = 266250 cm^3/h/g$_{cat}$ (STP) (W$_{cat}$ = 32 mg). T = 190 – 600°C, heating rate = 15°C/min.

$ZCu^{2+}(OH)^-$ and one Brønsted acid site, both characterized by single NH_3 bonds, thus conserving the overall NH_3 storage capacity. These findings comply well with previous literature results, where the monotonic decreasing trend of the Bronsted to Lewis NH_3 was observed upon aging, in correspondence to an approximately constant ammonia inventory under mild HTA conditions [17,18,28,51].

To evaluate the Lewis-NH_3/Cu^{2+} ratio, it is necessary to discriminate the different acid site contributions during the TPD process. Following a simplified approach used in the literature, a Gaussian deconvolution process has been adopted assuming two NH_3 adsorption sites [29]. The profiles obtained relying on such a technique are shown in Fig. 5 – B and Fig. 5 – C respectively for the *Degreened* and the *Aged* catalysts: notice that the cumulative curves result in close agreement with the experimental data, with an adjusted R-squared higher than 0.99 for both. The integrals from the deconvolution process are reported in Table SI.4, with negligible deviations from the experimental NH_3 release (~1%). The *Aged* Lewis-NH_3 is higher than the *Degreened* counterpart, indicative of the increased Z_2Cu^{2+} content due to the HTA process. The knowledge of the Lewis acid site population and of the reducible Cu^{2+} content enables the direct assessment of the Lewis-NH_3/Cu^{2+} ratio, reported in Table 4. These estimates are compared to the expected ratios computed using the Cu^{2+} speciation from the NO_2 adsorption tests, computed as $1*[ZCu^{2+}(OH)^-] + 2*[Z_2Cu^{2+}]$: a good agreement between the two is observed, confirming the adequacy of the previous ion population assessment.

The minor deviations between the ratios could be ascribed to the adoption of the gaussian function, not necessarily representative of the desorption process, and to the proximity of the two desorption peaks which may lead to over/under-estimations during the deconvolution. Similar considerations can be extended to the relative change of the peak intensity. The analyzed hydrothermal aging chemistry (1) implies an equimolar change between the Lewis and Bronsted NH_3, whereas considering the measured values (Table SI.4), the *Aged* ~4 μmol Lewis increment occurs concurrent to an excessive Bronsted loss of ~6 μmol. The limited difference (~2 μmol) can similarly be a deconvolution artifact, however a minor dealumination of the catalyst cannot be excluded.

3.3. Cu^{2+} nuclearity

Earlier in this manuscript (*Section 3.1*) we discussed the possible formation of binuclear Cu^{2+} species (Two-P) during the low-T SCR-RHC (2). This specific topic, and the relative HTA effect, is addressed here relying on the application of the transient CO to CO_2 oxidation employed as a probe reaction for Cu^{2+}-dimers. Previous works have assessed the validity of such a technique utilizing both kinetic analysis on the transient CO_2 release and in-situ UV–vis methods [34,37–39,46,54,55]. The requirements of a two-electrons transfer, and an oxygen-provider species, imply the involvement of a complex where two isolated $ZCu^{2+}(OH)^-$ ions serve as its precursors. Once a cations pair becomes NH_3-solvated, a Two-P complex is proposed to be formed according to (2), which acts as the catalytic active centre for the CO oxidation process. This has been highlighted in the works of some of us where the addition of a NH_3 saturation step, prior to the CO feed, induced a net enhancement of the CO_2 production [38,39]. The dual-site CO oxidation mechanism over the Two-P structure results as follows (6) [37,39].
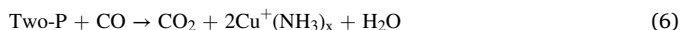
$$Two\text{-}P + CO \rightarrow CO_2 + 2Cu^+(NH_3)_x + H_2O \quad (6)$$

Table 4
Lewis-NH_3/Cu^{2+} ratios: comparison between the assessments from NO_2 adsorption tests and NH_3-TPDs deconvolution.

Sample	Lewis-NH_3/Cu^{2+} (NO_2 adsorption)	Lewis-NH_3/Cu^{2+} (deconvolution of NH_3 TPD)
Degreened	1.25	1.15
Aged	1.61	1.50

Thus, the CO_2 release can be directly associated to the presence of binuclear Cu^{2+} complexes (Two-P) in the zeolite cages. To maximize their formation, the considered CO oxidation protocols herein performed incorporate an NH_3 pre-adsorption step. The carbon dioxide release during the dry CO oxidation phase of the related protocol is depicted in Fig. 6 – A for both the *Degreened* and the *Aged* catalyst.

Like the N_2 trace during RHC transients, an initial CO_2 peak is observed at the CO step feed, followed by a slow monotonic decrease. A much greater CO_2 production is noted over the *Degreened* sample, being populated by more Two-P precursors ($ZCu^{2+}(OH)^-$) compared to the *Aged* catalyst, in accordance with the HTA sites transformation. A more than doubled integral carbon dioxide release is evaluated and reported in Table SI.5. Considering a 1:2 molar ratio between CO_2 and the $ZCu^{2+}(OH)^-$ content, it is possible to evaluate the extent of $ZCu^{2+}(OH)^-$ reduction: a higher reduced fraction is evaluated on the *Degreened* catalyst with respect to the *Aged* one as reported in Table 5 (~60% to ~50%), coherent with the kinetic dependency of the CO oxidation rate on the cation density [37,38]. Likewise, the Cu^{2+} reduction extent has been measured (Table 5): ~45% and 20% of Cu^{2+} sites are titrated on the *Degreened* and *Aged* samples, respectively. To verify such an occurrence, a $NO+NH_3$ co-feed step was performed in succession to the CO oxidation to close the Cu balance, confirming the different residual Cu^{2+} fractions for the two catalysts (Table SI.6). A more pronounced NO consumption (or N_2 production) over the *Aged* sample suggests a higher Cu^{2+} oxidation state, in agreement with the more limited reduction during the CO exposure. The global copper balance, accounting for the contribution of the two reduction phases, was verified for both samples with modest experimental error.

Due to the slow CO oxidation kinetics, a complete conversion was not observed during 90 min of CO exposure for both catalysts, similar to previous results [34,37,38], nevertheless, the maximum CO_2 production can be asymptotically estimated. A rate expression for the carbon dioxide release quadratic in the $ZCu^{2+}(OH)^-$ fraction was previously developed and, by proper integration adopting differential reactor conditions (in view of the very scarce CO conversion), a function describing the overall CO_2 evolution was derived (7) [34,37].

$$CO_{2,integral} = \frac{[Cu^{2+}]_0}{2} * \frac{2 * k_{app} * [Cu^{2+}]_0 * t}{1 + 2 * k_{app} * [Cu^{2+}]_0 * t} \quad (7)$$

Here $[Cu^{2+}]_0$ indicates the initial ions population, prior to the CO injection. This simple kinetic model was previously employed on model Cu-CHA catalysts, resulting in an effective description of the transient carbon dioxide release. Furthermore, the evaluation of its asymptote ($t\rightarrow\infty$) enabled to easily assess the maximum level of CO_2 production ($[Cu^{2+}]_0/2$) [34,37]. Fig. 6 – B depicts the application of the same model to the integral CO_2 traces collected over the state-of-the-art catalysts herein considered, showcasing the theoretical behavior across a wider time frame than the CO oxidation phase duration (adj. R^2 >0.99). The asymptotic limits (Table 5), counted twice according to the stoichiometry of the considered mechanism (6), resulted in good agreement with the different $ZCu^{2+}(OH)^-$ fractions assessed previously for the two samples through NO_2 adsorption/TPD tests. This finding further confirms that only $ZCu^{2+}(OH)^-$ sites are involved in the formation of Cu^{2+} dimers (or Two-P), thus enabling to clearly detect the occurrence of HTA under dry conditions. In fact, in the absence of H_2O in the feed stream, no $ZCu^{2+}(OH)^-$ hydrolysis (3) is expected to occur during CO oxidation, since H_2O formation would be very scarce and characterized by very limited rates [34,37], so that the $ZCu^{2+}(OH)^-$ cations content would not be essentially altered by (3).

Conditions more emblematic of real-world NH_3-SCR conditions were studied by replicating the CO oxidation protocol in the presence of 5% v/v H_2O. The corresponding carbon dioxide traces are shown in Fig. 7 – A.

A significant finding, not reported elsewhere, is the superimposed CO_2 release from the two catalysts, which points to a negligible aging
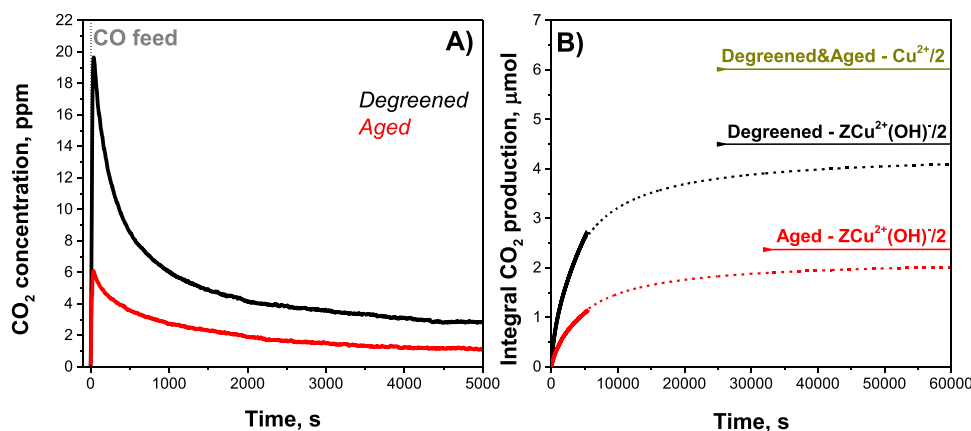
Fig. 6. CO oxidation phase, without water: transient (A) and integral (B) CO_2 production. The model prediction (7) is reported as dotted lines (B). Gas phase composition: $NH_3 = NO = 0$ ppm, $CO = 1000$ ppm, $O_2 = 0$ % v/v, $H_2O = 0$% v/v, balance He. GHSV = 266250 $cm^3/h/g_{cat}$ (STP) ($W_{cat} = 32$ mg). T = 200°C.

Table 5
Transient CO oxidation protocol: $ZCu^{2+}(OH)^-$ and Cu^{2+} reduction extents. Twice the theoretical CO_2 integral production, evaluated with (7), is alongside reported.

Protocol	Sample	$ZCu^{2+}(OH)^-$ red., %	Cu^{2+}red., %	2*Asymptotic Integral CO_2, μmol
Dry	*Degreened*	60.4	45.3	8.7
	Aged	50.6	19.8	4.4
Wet	*Degreened*	\	47.5	11.6
	Aged	\	47.8	12.3

effect. Consequently, identical Cu^{2+} reduction extents are evaluated, both during the CO exposure and during the closing NO + NH_3 RHC phase, remarking the identical behavior of the two samples (Table 5 and Table SI.6). As in the absence of water, the integral CO_2 productions were fitted by the 2nd order rate model (7) (adj. R^2 >0.9999), and the temporal evolutions of the integral CO_2 are displayed in Fig. 7 – B, resulting again in close trends for the two samples. At variance with the results in dry conditions, the new predicted asymptotes (Table 5) are now in close agreement with the overall Cu content of both catalysts. As the CO oxidation has been shown to proceed involving the coupling of $ZCu^{2+}(OH)^-$ species, these results provide solid evidence of the hydrolysis reaction (3). As all Cu^{2+} sites are converted into $ZCu^{2+}(OH)$, in fact, the whole copper loading partakes in the process: being characterized by similar Cu contents, the catalyst behaviours now become identical,

forming comparable amounts of Two-P, consistent with the RHC dynamics previously observed in the presence of pre-stored NH_3.

In addition to the present discussion, the observations related to the HTA effect and hydrolysis have been further consolidated by applying a 2nd order kinetic analysis previously developed for dry CO oxidation tests [38]. The results and the related discussion are reported in the Supporting Information (Section *SI4)*.

In conclusion, the transient CO oxidation protocol has a twofold application. In dry conditions, it enables to titrate the $ZCu^{2+}(OH)^-$ species, thus providing a method alternative to NO_2 and NH_3 adsorption/TPD tests to monitor modifications of the Cu speciation in Cu-CHA, based on the extrapolation of the 2nd order rate model for the integral CO_2 release [34,37]. If executed in the presence of H_2O, instead, the same 2nd order fit enables to count the overall reducible Cu^{2+} content [34,37]. Furthermore, the CO oxidation results lend further support to a Cu-pair mediated interpretation of the low-T Standard SCR redox mechanism [32–35,38,39].

4. Conclusions

This research has been dedicated to the investigation of HTA effects on Cu^{2+} ions (i.e., $ZCu^{2+}(OH)^-$ and Z_2Cu^{2+}) in state-of-the-art Cu-SSZ-13 catalysts for vehicular NH_3-SCR applications. This subject has been addressed adopting TRMs previously developed, and optimized, for characterization of model Cu-CHA materials. Two samples with similar composition yet different HTA extents (*Degreened* and *Aged*) have been studied: the main conclusions are summarized as follows.
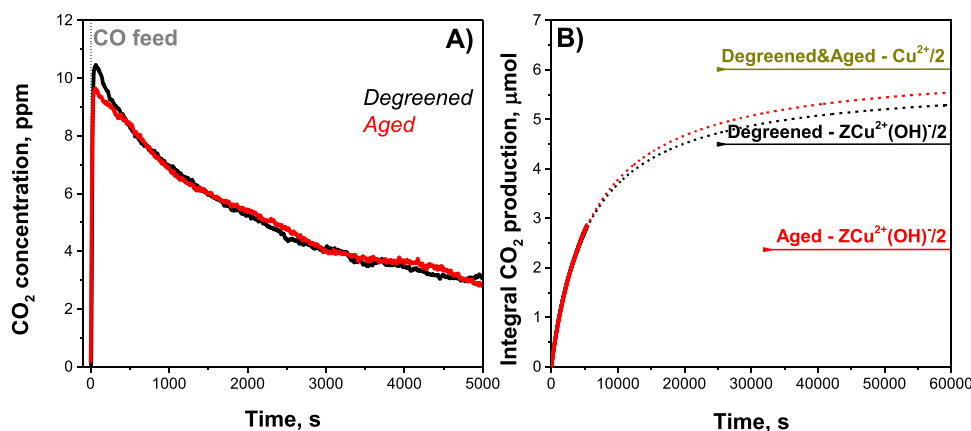

Fig. 7. CO oxidation phase, with H_2O: transient (A) and integral (B) CO_2 production. The model prediction (7) is reported as dotted lines (B). Gas phase composition: $NH_3 = NO = 0$ ppm, $CO = 1000$ ppm, $O_2 = 0$ % v/v, $H_2O = 5$ % v/v, balance He. GHSV = 266250 $cm^3/h/g_{cat}$ (STP) ($W_{cat} = 32$ mg). T = 200°C.

The overall reducible Cu^{2+} fraction remains invariant and independent of the HTA level. Isothermal $NO+NH_3$ reduction tests (with pre-stored NH_3) and ICP-MS measurements converge to titrate similar Cu loadings for both samples, implying negligible aging impact. The water presence does not hinder the quantification, however once fed a similar inhibition effect on the reduction dynamics is clearly observed for both samples, in agreement with a recent DFT study [49].

A modification of the Cu^{2+} speciation upon aging is conversely inferred from TPD analysis, successive to NO_2 and NH_3 isothermal adsorption. A decline in the $ZCu^{2+}(OH)^-$ population is measured upon aging during NO_2-TPDs, and the lower NO_2 desorption over the *Aged* sample is proposed to directly reflect the reduced content of such ions. Notably, similar quantifications are retrieved after several reduction/oxidation cycles, suggesting a lasting stability of the Cu^{2+} speciation if HTA conditions are not triggered. A $ZCu^{2+}(OH)^-$ decrement during HTA, concurrent with an increasing Z_2Cu^{2+} fraction and a consumption of Brønsted acid sites, is pointed out by NH_3-TPDs: the enhanced low-T feature of the *Aged* catalyst reconciles well with the greater NH_3 solvation extent of Cu cations characteristic of growing Z_2Cu^{2+} content. A deconvolution of these profiles reasonably confirms the cations populations counted by NO_2 adsorption/TPD.

The nuclearity of Cu^{2+} during conditions representative of the low-T regime of SCR-RHC has been probed by CO transient oxidation tests. Binuclear complexes (Two-P), originating from $ZCu^{2+}(OH)^-$, are considered to act as the reaction catalytic centers. In the absence of water, an evident reduction in the CO_2 production is observed over the *Aged* sample, consistent with the change in the nature of Cu^{2+} ions upon aging and highlighting this technique as an additional method to characterize the HTA and the related effects on Cu^{2+} speciation. Conversely, in the presence of H_2O, overlapping CO_2 profiles are observed for the two catalysts, irrespective of aging. This phenomenon can be ascribed to an NH_3 assisted hydrolysis reaction where Z_2Cu^{2+} species are reversibly converted to $ZCu^{2+}(OH)^-$, thus forming an equal amount of Cu^{2+} dimers over both catalysts, and therefore curtailing the HTA effect. This well agrees with the similar reduction dynamics detected during $NO+NH_3$ titration tests, where the pre-adsorbed NH_3 and the H_2O produced in-situ can also activate such a hydrolysis step and the related sites conversion.

The coherent results from the experimental protocols herein applied provide direct evidence for the Cu^{2+} speciation variation upon hydrothermal aging and are rationalized by the simple global transformation mechanism already proposed in literature ($ZCu^{2+}(OH)^- + ZH^+ \rightarrow Z_2Cu^{2+} + H_2O$). Albeit some results have been already reported in scattered research, this work extends and strengthens them proposing a systematic approach to the study of HTA. In addition, the evidence for the binuclear Cu^{2+} structure formation and complete sites hydrolysis supports recent findings on the dual-site nature of the low-T SCR-RHC on Cu-CHA catalysts, in contrast to RHC single site mechanisms.

We have herein demonstrated that a combination of simple well established transient response methods, previously proposed for model experimental catalysts, enables an effective, consistent, and direct characterization of the Cu^{2+} species also in the case of commercial Cu-CHA catalysts, in alternative to more sophisticated spectroscopic techniques commonly adopted in the literature. This research acts as a foundation for further investigations based on TRMs, aimed in particular at building structure-activity relations during hydrothermal aging phenomena by dissecting the analysis of the low-T STD-SCR reaction into distinct studies of the RHC and OHC [40,56].

Funding statements

CRediT authorship contribution statement

Umberto Iacobone: Writing – original draft, Validation, Investigation, Formal analysis. **Nicole Daniela Nasello:** Writing – review & editing, Visualization. **Isabella Nova:** Writing – review & editing, Supervision, Resources, Conceptualization. **Enrico Tronconi:** Writing – review & editing, Supervision, Project administration, Funding acquisition, Conceptualization. **Rohil Daya:** Writing – review & editing, Supervision, Resources, Project administration, Funding acquisition, Data curation. **Hongmei An:** Writing – review & editing, Resources. **Unmesh Menon:** Writing – review & editing.

Declaration of Competing Interest

The authors declare that they have no known competing financial interests or personal relationships that could have appeared to influence the work reported in this paper.

Data availability

The data that has been used is confidential.

Appendix A. Supporting information

Supplementary data associated with this article can be found in the online version at doi:10.1016/j.apcatb.2024.123989.

References

[1] K. Skalska, J.S. Miller, S. Ledakowicz, Trends in NOx abatement: a review, Sci. Total Environ. 408 (2010) 3976–3989, https://doi.org/10.1016/j.scitotenv.2010.06.001.

[2] E. Mulholland, J. Miller, Y. Bernard, K. Lee, F. Rodríguez, The role of NOx emission reductions in Euro 7 / VII vehicle emission standards to reduce adverse health impacts in the EU27 through 2050, Transp. Eng. 9 (2022) 100133, https://doi.org/10.1016/j.treng.2022.100133.

[3] R. Daya, Emission control of nitrogen oxides—current status and future challenges, SAE Int. J. Sustain. Transp., Energy, Environ., Policy 2 (2021) 121–139, https://doi.org/10.4271/13-02-02-0008.

[4] E. Borfecchia, P. Beato, S. Svelle, U. Olsbye, C. Lamberti, S. Bordiga, Cu-CHA-a model system for applied selective redox catalysis, Chem. Soc. Rev. 47 (2018) 8097–8133, https://doi.org/10.1039/c8cs00373d.

[5] F. Gao, J. Szanyi, On the hydrothermal stability of Cu/SSZ-13 SCR catalysts, Appl. Catal. A Gen. 560 (2018) 185–194, https://doi.org/10.1016/j.apcata.2018.04.040.

[6] K. Leistner, O. Mihai, K. Wijayanti, A. Kumar, K. Kamasamudram, N.W. Currier, A. Yezerets, L. Olsson, Comparison of Cu/BEA, Cu/SSZ-13 and Cu/SAPO-34 for ammonia-SCR reactions, Catal. Today 258 (2015) 49–55, https://doi.org/10.1016/j.cattod.2015.04.004.

[7] M.P. Ruggeri, I. Nova, E. Tronconi, J.E. Collier, A.P.E. York, Structure–activity relationship of different Cu–zeolite catalysts for NH_3–SCR, Top. Catal. 59 (2016) 875–881, https://doi.org/10.1007/s11244-016-0562-6.

[8] J.H. Kwak, R.G. Tonkyn, D.H. Kim, J. Szanyi, C.H.F. Peden, Excellent activity and selectivity of Cu-SSZ-13 in the selective catalytic reduction of NOx with NH_3, J. Catal. 275 (2010) 187–190, https://doi.org/10.1016/j.jcat.2010.07.031.

[9] P.G. Blakeman, E.M. Burkholder, H.Y. Chen, J.E. Collier, J.M. Fedeyko, H. Jobson, R.R. Rajaram, The role of pore size on the thermal stability of zeolite supported Cu SCR catalysts, Catal. Today 231 (2014) 56–63, https://doi.org/10.1016/j.cattod.2013.10.047.

[10] J.H. Kwak, D. Tran, S.D. Burton, J. Szanyi, J.H. Lee, C.H.F. Peden, Effects of hydrothermal aging on NH_3-SCR reaction over Cu/zeolites, J. Catal. 287 (2012) 203–209, https://doi.org/10.1016/j.jcat.2011.12.025.

[11] I. Nova E. Tronconi Urea-SCR Technology for deNOx After Treatment of Diesel Exhaust, 2014 doi: 10.1007/978-1-4899-8071-7.

[12] C. Paolucci, I. Khurana, A.A. Parekh, S. Li, A.J. Shih, H. Li, J.R. Di Iorio, J. D. Albarracin-Caballero, A. Yezerets, J.T. Miller, W.N. Delgass, F.H. Ribeiro, W. F. Schneider, R. Gounder, Dynamic multinuclear sites formed by mobilized copper ions in NOx selective catalytic reduction, Science 357 (2017) 898–903, https://doi.org/10.1126/science.aan5630.

[13] C. Liu, H. Kubota, T. Amada, K. Kon, T. Toyao, Z. Maeno, K. Ueda, J. Ohyama, A. Satsuma, T. Tanigawa, N. Tsunoji, T. Sano, K. ichi Shimizu, In SItu Spectroscopic Studies on the Redox Cycle of NH_3−SCR over Cu−CHA zeolites, ChemCatChem 12 (2020) 3050–3059, https://doi.org/10.1002/cctc.202000024.

[14] W.P. Partridge, S.Y. Joshi, J.A. Pihl, N.W. Currier, New operando method for quantifying the relative half-cycle rates of the NO SCR redox cycle over Cu-exchanged zeolites, Appl. Catal. B 236 (2018) 195–204, https://doi.org/10.1016/j.apcatb.2018.04.071.

[15] J.H. Kwak, H. Zhu, J.H. Lee, C.H.F. Peden, J. Szanyi, Two different cationic positions in Cu-SSZ-13, Chem. Commun. 48 (2012) 4758–4760, https://doi.org/10.1039/c2cc31184d.

[16] J. Luo, H. An, K. Kamasamudram, N. Currier, A. Yezerets, T. Watkins, L. Allard, Impact of accelerated hydrothermal aging on structure and performance of Cu-SSZ-

13 SCR catalysts, SAE Int J. Engines 8 (2015) 1181–1186, https://doi.org/10.4271/2015-01-1022.

[17] R. Villamaina, S. Liu, I. Nova, E. Tronconi, M.P. Ruggeri, J. Collier, A. York, D. Thompsett, Speciation of Cu cations in Cu-CHA catalysts for NH$_3$-SCR: effects of SiO$_2$/Al$_2$O$_3$ ratio and Cu-loading investigated by transient response methods, ACS Catal. 9 (2019) 8916–8927, https://doi.org/10.1021/acscatal.9b02578.

[18] J. Luo, F. Gao, K. Kamasamudram, N. Currier, C.H.F. Peden, A. Yezerets, New insights into Cu/SSZ-13 SCR catalyst acidity. Part I: nature of acidic sites probed by NH$_3$ titration, J. Catal. 348 (2017) 291–299, https://doi.org/10.1016/j.jcat.2017.02.025.

[19] C. Paolucci, A.A. Parekh, I. Khurana, J.R. Di Iorio, H. Li, J.D. Albarracin Caballero, A.J. Shih, T. Anggara, W.N. Delgass, J.T. Miller, F.H. Ribeiro, R. Gounder, W. F. Schneider, Catalysis in a cage: condition-dependent speciation and dynamics of exchanged cu cations in SSZ-13 zeolites, J. Am. Chem. Soc. 138 (2016) 6028–6048, https://doi.org/10.1021/jacs.6b02651.

[20] J. Luo, D. Wang, A. Kumar, J. Li, K. Kamasamudram, N. Currier, A. Yezerets, Identification of two types of Cu sites in Cu/SSZ-13 and their unique responses to hydrothermal aging and sulfur poisoning, Catal. Today 267 (2016) 3–9, https://doi.org/10.1016/j.cattod.2015.12.002.

[21] S.L. Bergman, S. Dahlin, V.V. Mesilov, Y. Xiao, J. Englund, S. Xi, C. Tang, M. Skoglundh, L.J. Pettersson, S.L. Bernasek, In-situ studies of oxidation/reduction of copper in Cu-CHA SCR catalysts: comparison of fresh and SO$_2$-poisoned catalysts, Appl. Catal. B 269 (2020) 118722, https://doi.org/10.1016/j.apcatb.2020.118722.

[22] Y. Jangjou, Q. Do, Y. Gu, L.G. Lim, H. Sun, D. Wang, A. Kumar, J. Li, L.C. Grabow, W.S. Epling, Nature of Cu active centers in Cu-SSZ-13 and their responses to SO$_2$ exposure, ACS Catal. 8 (2018) 1325–1337, https://doi.org/10.1021/acscatal.7b03095.

[23] D.J. Deka, R. Daya, A. Ladshaw, D. Trandal, S.Y. Joshi, W.P. Partridge, Assessing impact of real-world aging on Cu-redox half cycles of a Cu-SSZ-13 SCR catalyst via transient response measurements and kinetic modeling, Appl. Catal. B 309 (2022) 121233, https://doi.org/10.1016/j.apcatb.2022.121233.

[24] M. Valdez Lancinha Pereira, A. Nicolle, D. Berthout, Hydrothermal aging effects on Cu-zeolite NH$_3$-SCR catalyst, Catal. Today 258 (2015) 424–431, https://doi.org/10.1016/j.cattod.2015.03.027.

[25] D. Wang, Y. Jangjou, Y. Liu, M.K. Sharma, J. Luo, J. Li, K. Kamasamudram, W. S. Epling, A comparison of hydrothermal aging effects on NH$_3$-SCR of NOx over Cu-SSZ-13 and Cu-SAPO-34 catalysts, Appl. Catal. B 165 (2015) 438–445, https://doi.org/10.1016/j.apcatb.2014.10.020.

[26] S.J. Schmieg, S.H. Oh, C.H. Kim, D.B. Brown, J.H. Lee, C.H.F. Peden, D.H. Kim, Thermal durability of Cu-CHA NH$_3$-SCR catalysts for diesel NOx reduction, Catal. Today 184 (2012) 252–261, https://doi.org/10.1016/j.cattod.2011.10.034.

[27] S. Han, Q. Ye, S. Cheng, T. Kang, H. Dai, Effect of the hydrothermal aging temperature and Cu/Al ratio on the hydrothermal stability of CuSSZ-13 catalysts for NH$_3$-SCR, Catal. Sci. Technol. 7 (2017) 703–717, https://doi.org/10.1039/c6cy02555b.

[28] Y. Wu, T. Andana, Y. Wang, Y. Chen, E.D. Walter, M.H. Engelhard, K.G. Rappé, Y. Wang, F. Gao, U. Menon, R. Daya, D. Trandal, H. An, Y. Zha, K. Kamasamudram, A comparative study between real-world and laboratory accelerated aging of Cu/SSZ-13 SCR catalysts, Appl. Catal. B 318 (2022) 121807, https://doi.org/10.1016/j.apcatb.2022.121807.

[29] J. Luo, K. Kamasamudram, N. Currier, A. Yezerets, NH3-TPD methodology for quantifying hydrothermal aging of Cu/SSZ-13 SCR catalysts, Chem. Eng. Sci. 190 (2018) 60–67, https://doi.org/10.1016/j.ces.2018.06.015.

[30] A. Martini, E. Borfecchia, K.A. Lomachenko, I.A. Pankin, C. Negri, G. Berlier, P. Beato, H. Falsig, S. Bordiga, C. Lamberti, Composition-driven Cu-speciation and reducibility in Cu-CHA zeolite catalysts: a multivariate XAS/FTIR approach to complexity, Chem. Sci. 8 (2017) 6836–6851, https://doi.org/10.1039/c7sc02266b.

[31] A. Godiksen, F.N. Stappen, P.N.R. Vennestrøm, F. Giordanino, S.B. Rasmussen, L. F. Lundegaard, S. Mossin, Coordination environment of copper sites in Cu-CHA zeolite investigated by electron paramagnetic resonance, J. Phys. Chem. C. 118 (2014) 23126–23138, https://doi.org/10.1021/jp5065616.

[32] W. Hu, T. Selleri, F. Gramigni, E. Fenes, K.R. Rout, S. Liu, I. Nova, D. Chen, X. Gao, E. Tronconi, On the redox mechanism of low-temperature NH$_3$-SCR over Cu-CHA: a combined experimental and theoretical study of the reduction half cycle, Angew. Chem. 133 (2021) 7273–7280, https://doi.org/10.1002/ange.202014926.

[33] F. Gramigni, N.D. Nasello, N. Usberti, U. Iacobone, T. Selleri, W. Hu, S. Liu, X. Gao, I. Nova, E. Tronconi, Transient kinetic analysis of low-temperature NH$_3$-SCR over Cu-CHA catalysts reveals a quadratic dependence of Cu reduction rates on Cu^{II}, ACS Catal. 11 (2021) 4821–4831, https://doi.org/10.1021/acscatal.0c05362.

[34] W. Hu, U. Iacobone, F. Gramigni, Y. Zhang, X. Wang, S. Liu, C. Zheng, I. Nova, X. Gao, E. Tronconi, Unraveling the hydrolysis of Z$_2$Cu^{2+} to ZCu^{2+}(OH)$^-$ and its consequences for the low-temperature selective catalytic reduction of NO on Cu-CHA catalysts, ACS Catal. 11 (2021) 11616–11625, https://doi.org/10.1021/acscatal.1c02761.

[35] N. Usberti, F. Gramigni, N.D. Nasello, U. Iacobone, T. Selleri, W. Hu, S. Liu, X. Gao, I. Nova, E. Tronconi, An experimental and modelling study of the reactivity of adsorbed NH$_3$ in the low temperature NH$_3$-SCR reduction half-cycle over a Cu-CHA catalyst, Appl. Catal. B 279 (2020) 119397, https://doi.org/10.1016/j.apcatb.2020.119397.

[36] R. Villamaina, F. Gramigni, U. Iacobone, S. Liu, I. Nova, E. Tronconi, M.P. Ruggeri, J. Collier, A.P.E. York, D. Thompsett, The H$_2$O effect on Cu speciation in Cu-CHA-

catalysts for NH$_3$-SCR probed by NH$_3$ titration, Catalysts 11 (2021) 759, https://doi.org/10.3390/catal11070759.

[37] U. Iacobone, I. Nova, E. Tronconi, R. Villamaina, M.P. Ruggeri, J. Collier, D. Thompsett, Transient CO oxidation as a versatile technique to investigate Cu^{2+} titration, speciation and sites hydrolysis on Cu–CHA catalysts: the Cu loading effect, Top. Catal. 66 (2023) 761–770, https://doi.org/10.1007/s11244-023-01813-8.

[38] R. Villamaina, U. Iacobone, I. Nova, M.P. Ruggeri, J. Collier, D. Thompsett, E. Tronconi, Low-T CO oxidation over Cu−CHA catalysts in presence of NH$_3$: probing the mobility of Cu^{II} ions and the role of multinuclear Cu^{II} species, ChemCatChem 12 (2020) 3843–3848, https://doi.org/10.1002/cctc.202000734.

[39] U. Iacobone, I. Nova, E. Tronconi, R. Villamaina, M.P. Ruggeri, J. Collier, D. Thompsett, Appraising multinuclear Cu^{2+} structure formation in Cu-CHA SCR catalysts via low-T dry CO oxidation with modulated NH$_3$ solvation, ChemistryOpen 11 (2022) e202200186, https://doi.org/10.1002/open.202200186.

[40] N.D. Nasello, N. Usberti, U. Iacobone, F. Gramigni, W. Hu, S. Liu, I. Nova, X. Gao, E. Tronconi, Dual-site RHC and OHC transient kinetics predict low-T standard SCR steady-state rates over a Cu-CHA catalyst, ACS Catal. 13 (2023) 2723–2734, https://doi.org/10.1021/acscatal.2c06071.

[41] D.J. Deka, R. Daya, A. Ladshaw, S.Y. Joshi, W.P. Partridge, A transient-response methodology based on experiments and modeling for Cu-redox half-cycle kinetic analysis on a Cu-SSZ-13 SCR catalyst, Chem. Eng. J. 435 (2022) 134219, https://doi.org/10.1016/j.cej.2021.134219.

[42] R. Daya, D. Trandal, R.K. Dadi, H. Li, S.Y. Joshi, J. Luo, A. Kumar, A. Yezerets, Kinetics and thermodynamics of ammonia solvation on Z$_2$Cu, ZCuOH and ZCu sites in Cu-SSZ-13 – implications for hydrothermal aging, Appl. Catal. B 297 (2021) 120444, https://doi.org/10.1016/j.apcatb.2021.120444.

[43] R. Daya, D. Trandal, U. Menon, D.J. Deka, W.P. Partridge, S.Y. Joshi, Kinetic model for the reduction of Cu^{II} Sites by NO + NH$_3$ and reoxidation of NH$_3$-solvated Cu^I sites by O$_2$ and NO in Cu-SSZ-13, ACS Catal. 12 (2022) 6418–6433, https://doi.org/10.1021/acscatal.2c01076.

[44] C. Negri, P.S. Hammershøi, T.V.W. Janssens, P. Beato, G. Berlier, S. Bordiga, Investigating the low temperature formation of Cu^{II}-(N,O) species on Cu-CHA zeolites for the selective catalytic reduction of NOx, Chem. - A Eur. J. 24 (2018) 12044–12053, https://doi.org/10.1002/chem.201802769.

[45] F. Gao, C.H.F. Peden, Recent progress in atomic-level understanding of Cu/SSZ-13 selective catalytic reduction catalysts, Catalysts 8 (2018) 140, https://doi.org/10.3390/catal8040140.

[46] C. Paolucci, J.R. Di Iorio, W.F. Schneider, R. Gounder, Solvation and mobilization of copper active sites in zeolites by ammonia: consequences for the catalytic reduction of nitrogen oxides, Acc. Chem. Res 53 (2020) 1881–1892, https://doi.org/10.1021/acs.accounts.0c00328.

[47] C. Paolucci, A.A. Verma, S.A. Bates, V.F. Kispersky, J.T. Miller, R. Gounder, W. N. Delgass, F.H. Ribeiro, W.F. Schneider, Isolation of the copper redox steps in the standard selective catalytic reduction on Cu-SSZ-13, Angew. Chem. - Int. Ed. 53 (2014) 11828–11833, https://doi.org/10.1002/anie.201407030.

[48] N. Ottinger, Y. Xi, C. Keturakis, Z.G. LiuImpact of Water Vapor on the Performance of a Cu-SSZ-13 Catalyst under Simulated Diesel Exhaust Conditions SAE Technical Papers , 2021, , 2872–2877, 10.4271/2021-01-0577.

[49] G. Contaldo, M. Ferri, C. Negri, I. Nova, M. Maestri, E. Tronconi, First-principles assessment of the role of water in the reduction half cycle of low-temperature NH$_3$-SCR over Cu-CHA, ChemCatChem 15 (2023) e2023006, https://doi.org/10.1002/cctc.202300673.

[50] M. Colombo, I. Nova, E. Tronconi, NO$_2$ adsorption on Fe- and Cu-zeolite catalysts: the effect of the catalyst red-ox state, Appl. Catal. B 111 112 (2012) 433–444, https://doi.org/10.1016/j.apcatb.2011.10.031.

[51] J. Luo, K. Kamasamudram, N. Currier, A. Yezerets, NH$_3$-TPD methodology for quantifying hydrothermal aging of Cu/SSZ-13 SCR catalysts, Chem. Eng. Sci. 190 (2018) 60–67, https://doi.org/10.1016/j.ces.2018.06.015.

[52] E. Borfecchia, C. Negri, K.A. Lomachenko, C. Lamberti, T.V.W. Janssens, G. Berlier, Temperature-dependent dynamics of NH$_3$-derived Cu species in the Cu-CHA SCR catalyst, React. Chem. Eng. 4 (2019) 1067–1080, https://doi.org/10.1039/c8re00322j.

[53] F. Giordanino, E. Borfecchia, K.A. Lomachenko, A. Lazzarini, G. Agostini, E. Gallo, A.V. Soldatov, P. Beato, S. Bordiga, C. Lamberti, Interaction of NH$_3$ with Cu-SSZ-13 catalyst: A complementary FTIR, XANES, and XES study, J. Phys. Chem. Lett. 5 (2014) 1552–1559, https://doi.org/10.1021/jz500241m.

[54] P. Da Costa, B. Modén, G.D. Meitzner, D.K. Lee, E. Iglesia, Spectroscopic and chemical characterization of active and inactive Cu species in NO decomposition catalysts based on Cu-ZSM5, Phys. Chem. Chem. Phys. 4 (2002) 4590–4601, https://doi.org/10.1039/b203700a.

[55] W. Hu, F. Gramigni, N.D. Nasello, U. Usberti, S. Liu, I. Nova, X. Gao, E. Tronconi, Dynamic binuclear cuiisites in the reduction half-cycle of low-temperature NH$_3$-SCR over Cu-CHA catalysts, ACS Catal. 12 (2022) 5263–5274, https://doi.org/10.1021/acscatal.2c01213.

[56] N.D. Nasello, U. Iacobone, N. Usberti, A. Gjetja, I. Nova, E. Tronconi, R. Villamaina, M.P. Ruggeri, D. Bounechada, A.P.E. York, J. Collier, Investigation of low-temperature OHC and RHC in NH$_3$–SCR over Cu-CHA catalysts: effects of H$_2$O and SAR, ACS Catal. 14 (2024) 4265–4276, https://doi.org/10.1021/acscatal.4c00118.